A New Kinetic-Based Solver for Solving Compressible Flow on Arbitrary Polyhedral Grids

Li Shujie*, Yang Guowei

Key Laboratory of High Temperature Gas Dynamics, Institute of Mechanics, Chinese Academy of Sciences, Beijing 100190, China

Abstract

A kinetic-based unstructured algorithm for obtaining the numerical solution to three-dimensional, inviscid, compressible flows is developed and implemented on arbitrary polyhedral grids. The algorithm is derived using a cell-centered finite volume formulation for arbitrary grids topology including honeycomb grids. A new improved radical basis function method is proposed for the accurate and robust gradient calculation. The new method does not depend on the geometry of cell. Thus it is much less sensitive to the shape of the grid especially for honeycomb mesh. After an accurate gradient computation, the spatial second order accuracy is achieved through the MUSCL approach along with the Kinetic Flux Vector Splitting scheme. With a point implicit relaxation time marching strategy, the solver remains stable at large courant number for high Mach number computation. Several test cases are being conducted on the accuracy and efficiency of the solver. The model test cases include two-dimensional unstructured mesh scramjet inlets computation and three-dimensional multi-block structured mesh M6 wing test case. The further evolution of the performance on honeycomb grids simulation is investigated. Fast convergence of honeycomb based computation is observed as expected. The test cases indicate that the algorithms and the solver developed in this paper exhibit good flexibility on mesh universality and robustness for high speed flow simulation. Finally, the solver is applied to a three-dimensional aircraft configuration successfully.

Keywords polyhedral grids; compressible flow; Radical Basis Function; hypersonic flow; KFVS;

1. Introduction

Algorithms for solving compressible flow using unstructured grids have become popular in the CFD community, mainly because they offer the possibility of a much reduced grid generation effort for flows with complex geometry. Some of the pioneering work includes Jameson[1], Barth[2], Lo hner[3], Maviplis[4], and Frink[5] et al. However, one of the major disadvantages of unstructured solver is the lower accuracy. For this reason, hybrid element approach was proposed. In despite of that, unstructured or hybrid grids based solver is still less accurate than a structured grids solver, especially in hypersonic flow simulations.

This paper describes the algorithm of the XPOLY solver, which is a three-dimensional cell-centered finite volume compressible flow solver on arbitrary meshes. The objectives of this effort are to provide an accurate, robust flow field solution capability that can solve high speed problems containing complex shock wave structure flexibility on all types of meshes. These objectives require a solution algorithm that is forgiving of grids with different shapes of skewed elements. The algorithm must implement an accurate reconstructing process on arbitrary grids. The reconstruction includes face flux and gradient calculations. For face flux calculation, most of the classic approximation Riemann solvers suffer from unphysical problems. So some physical-based flux methods give us a light. Such as the Kinetic Flux Vector Splitting scheme (KFVS)[6] and the gas-kinetic BGK scheme[7]. For gradient calculation, Gauss-Green and Least Square Methods are popular. But Gauss-Green method performs badly on skewed elements while Least Square Method can not give a more accurate solution compared with the Gauss-Green method for structured grid calculation[8].

To overcome these difficulties, a new improved radial basis function gradient computation method along with a KFVS flux is proposed on general shapes of grids. Numerical validations are conducted on the accuracy and robustness of the new algorithms on different types of grids for compressible flows.

2. Reconstruction on Arbitrary Polyhedral Mesh

2.1 Kinetic flux vector splitting Scheme

The Kinetic Flux Vector Splitting (KFVS)[6] scheme is inspired from the kinetic theory of gases. There is a correspondence between the solution of the collision- less Boltzmann equation and the Euler equation.

$$\langle \psi, \partial_t f + \vec{u} \cdot \nabla^{\rightarrow} f \rangle = \partial_t U + \nabla \cdot F = 0 \qquad (1)$$

Where f is the Maxwellian-Boltzmann distribution function given by

* Corresponding author. *E-mail address:* xpoly. sj@gmail. com

Foundation item: Funded by The CAS Special Grant for Postgraduate Research, Innovation and Practice, 2010.

$$f=\rho\left(\frac{\lambda}{\pi}\right)^{3/2}e^{-\lambda[\|\vec{u}-\vec{v}\|^2+\xi^2]}, \quad (2)$$

The inner product $<\psi, f>$ is defined by

$$\langle\psi,f\rangle=\int\psi f\,\mathrm{d}u\mathrm{d}v\mathrm{d}w\mathrm{d}\xi \quad (3)$$

The conserved vector can be written as $U=<\psi, f>$ and $F=<\psi,\vec{u}f>$ is the flux vector of the Euler equations. Where

$$\psi=(1,u,v,w,\frac{1}{2}(u^2+v^2+w^2+\xi^2))^T \quad (4)$$

And u, v, w are the phase-space velocities. $\lambda=0.5\rho/p$. The variable ξ stands for the internal degrees of freedom.

Consider a cell-centered finite-volume discretization of the Euler equation, for cell I

$$\int_{V_I}\partial_t U\mathrm{d}V+\int_{\partial V_I}\vec{F}\cdot\mathrm{d}\vec{S}=0 \quad (5)$$

The flux F is the macro transport quantity of molecules random motions. At the surface of the cell, the flux is due to molecules coming from the left ($V_n>0$, here V_n is the normal velocity) with the state U_L and those from the right ($V_n<0$) with the state U_R. Hence the kinetic flux can be computed as

$$\int_{\partial V_I}\vec{F}\cdot\mathrm{d}\vec{S}=F^+ + F^-$$
$$F^+=\int_{\partial V_I}\int\int_0^\infty\vec{V}f\psi\mathrm{d}V_n\mathrm{d}\xi\mathrm{d}\vec{s}$$
$$F^-=\int_{\partial V_I}\int\int_{-\infty}^0\vec{V}f\psi\mathrm{d}V_n\mathrm{d}\xi\mathrm{d}\vec{s} \quad (6)$$

That is exactly the KFVS scheme [6]. The flux integral of Eq. (7) can be operated on arbitrary polyhedral grids and the resulted discretization of Eq. (5), (6) is solved by a point implicit time marching method similar to Gnoffo [9].

2.2 New gradient calculation method

In order to obtain second order spatial accuracy, cell gradient needs to be estimated. However, a less accurate gradient computational method usually leads to bad results or code crash. With general polyhedral grids, it is hard to control the mesh quality. These distorted grids on local neighbor stencil lead to a scattered data characteristic and make the classical gradient calculation method inaccurate and less robust. To overcome this problem, a new gradient calculation method is proposed in the frame of cell-centered finite volume method on polyhedral grids.

The new method is based on radical basis function method[10]. The radical basis functions method provides a very general and flexible way of interpolation in multi-dimensional spaces. Because of its good approximation properties, the method is a popular choice in many different areas. In this paper, the radial basis functions method is extended to the gradient calculation on arbitrary polyhedral grids.

Suppose that T is the function to be interpolated at the set $X=\{x_k\}_{k=1,N}$ on local cell neighbor stencil. Let ϕ be a basis function defined on the positive real axis. The interpolation space then consists of all functions of the form

$$S(\mathrm{x})=\sum_{k=1}^{N}\alpha_k\varphi(\|\mathrm{x}-\mathrm{x}_k\|)+\sum_{k=1}^{4}\beta_k d_k(\mathrm{x}) \quad (7)$$

Here $\|.\|$ denotes the standard Euclidean Norm. $d_k(x)=\{1, x, y, z \mid 1\le k\le 4\}$. The coefficient α_k and β_k are chosen so that S interpolates T exactly at the data points

$$S(\mathrm{x}_k)=T(\mathrm{x}_k),\ k=1,2,\ldots,N \quad (8)$$

And β_k must satisfy the side condition

$$\sum_{k=1}^{4}\beta_k d_k(\mathrm{x}_k)=0,\ k=1,2,\ldots,N \quad (9)$$

The basis function ϕ is chosen as multiquadrics (MQ) for its best performance

$$\varphi(r)=\sqrt{r^2+c^2},\ c>0 \quad (10)$$

In this paper, the free parameter c is given by Eq. (11). It performs well in all the test cases.

$$c=\frac{N}{\sum_{k=1}^{N}\frac{1}{r_k}} \quad (11)$$

The resulted linear equation system takes the form

$$\begin{pmatrix}\mathrm{A} & \mathrm{B}\\ \mathrm{B}^T & 0\end{pmatrix}\begin{pmatrix}\alpha\\ \beta\end{pmatrix}=\begin{pmatrix}\mathrm{T}\\ 0\end{pmatrix} \quad (12)$$

Where A is the basis matrix and B is first degree polynomials matrix

$$\mathrm{A}_{ij}=\varphi(\|x_i-x_j\|);B_{ij}=d_i(x_j), \quad (13)$$

Under the constrained conditions (8), (9) this system is non-singular, thus a unique solution exists. We notice that the $S(x)$ is differentiable, so it can be used to calculate $S'(x)$ in an arbitrary shape of grid meanwhile keeps the accurate interpolation properties of radical basis functions. The gradients of primitive quality q in the center of grid are given by

$$\nabla q(x_c)=\sum_{i=1}^{N}\alpha_i\nabla\varphi(\|x_c-x_i\|)+\sum_{i=1}^{4}\beta_i\nabla d_i(x_c) \quad (14)$$

After an accurate gradient computation, the spatial second order accuracy is achieved through the MUSCL approach along with the Kinetic Flux Vector Splitting scheme. Because of the point implicit relaxation strategy, the solver remains stable at large courant number without solving large linear systems meanwhile is able to maintain a good stability for high Mach number computation.

3. Numerical Results

3.1 Mach 3 scramjet intake

A mach 3 supersonic scramjet intake [11] is simulated on unstructured hexahedral grids. The grids are generated by extruding 2D unstructured quadrangle grids to 3D unstructured hexahedral grids. The local grids are shown in Fig. 1. A similar comparison between the XPOLY's (top) and Nakahashi's (bottom) solutions for the Mach number contours is shown in Fig. 2.

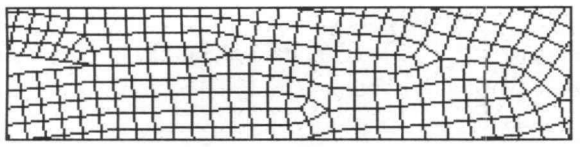

Fig. 1 Local grids of scramjet intake

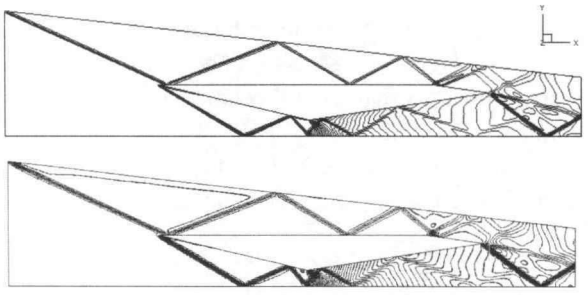

Fig. 2 Comparison of Mach number contours

3.2 ONERA M6 wing

The ONERA M6 wing [12] has been widely used as a standard test case for CFD solvers. This case is based on the multi-block structured meshes which are shown in Fig. 3. Results are computed at Mach number of 0.8395 and angle of attack of 3.06 degrees. As shown in Fig. 3, the lambda shock waves are well resolved. Surface pressure coefficient distributions at five spanwise cuts are compared with experimental data [11] in Fig. 4.

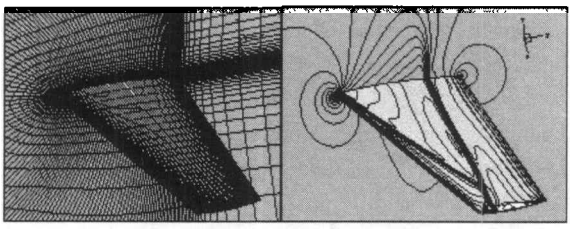

Fig. 3 Structured grids and surface pressure distribution

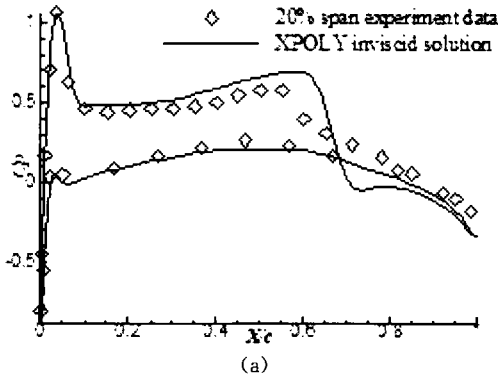

(a)

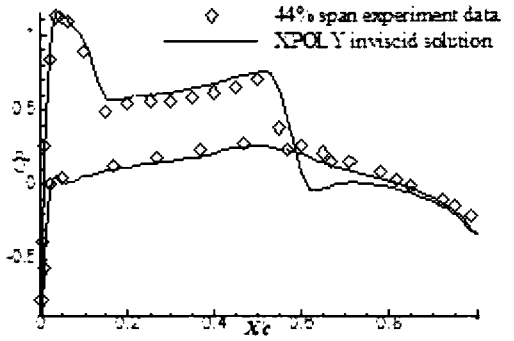

(b)

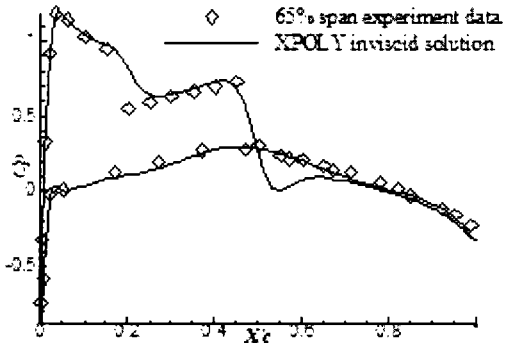

(c)

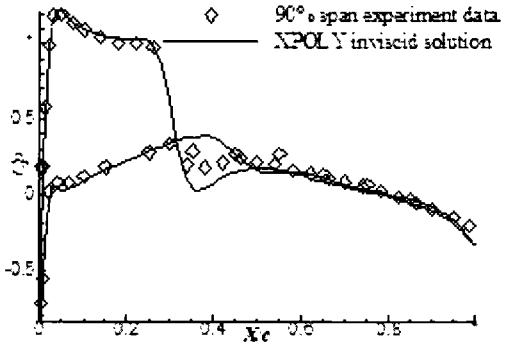

(d)

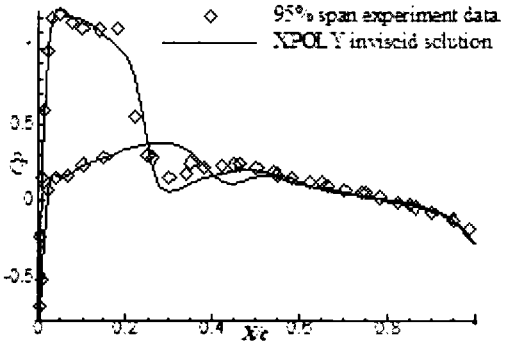

(e)

Fig. 4 Surface pressure distribution at five spanwise cuts

3.2 Honeycomb grids based computations

In this section, hypersonic flow around a double cone at Mach 15 is simulated on honeycomb grids aiming at the evolution of convergence of strong shock wave flow field computation. The double cone geometry is shown in reference [13]. The honeycomb grids are generated by connecting centroid-dual of the given mesh in Fig. 5. This procedure usually improved the quality of the

original grids.

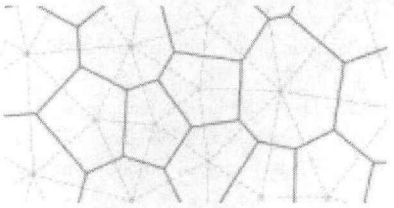

Fig. 5 Honeycomb grids obtained by using centroid-dual tessellations

Fig. 6 shows the honeycomb grids of the double cone. The Mach number contour and convergence history are shown in Fig. 7. The density residuals were reduced by seven orders of magnitude in less than 450 cycles, it is fast as we expected.

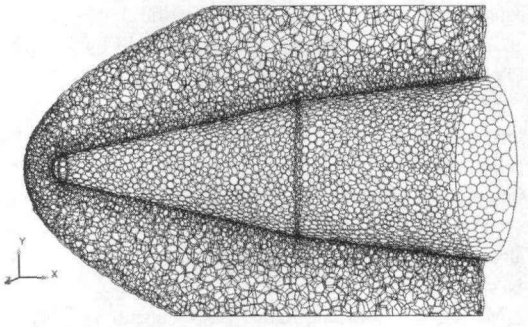

Fig. 6 Honeycomb grids of double cone geometry

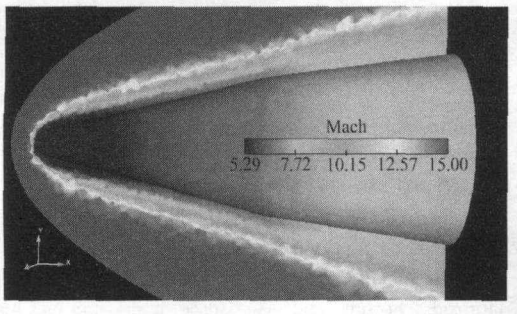

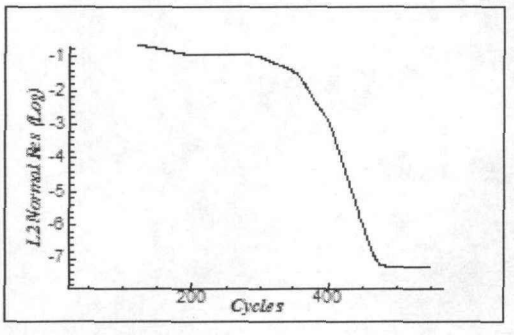

Fig. 7 Mach number contour and convergences history

3.3 Test of a whole aircraft

The computational capability of complex flow field is tested in this section. A whole aircraft flying at Mach number of 1.8 is simulated on the honeycomb grids. The aircraft geometry is similarly to the US F-18 fighter. Fig. 8 gives the three-view of honeycomb grids of the F-18 aircraft.

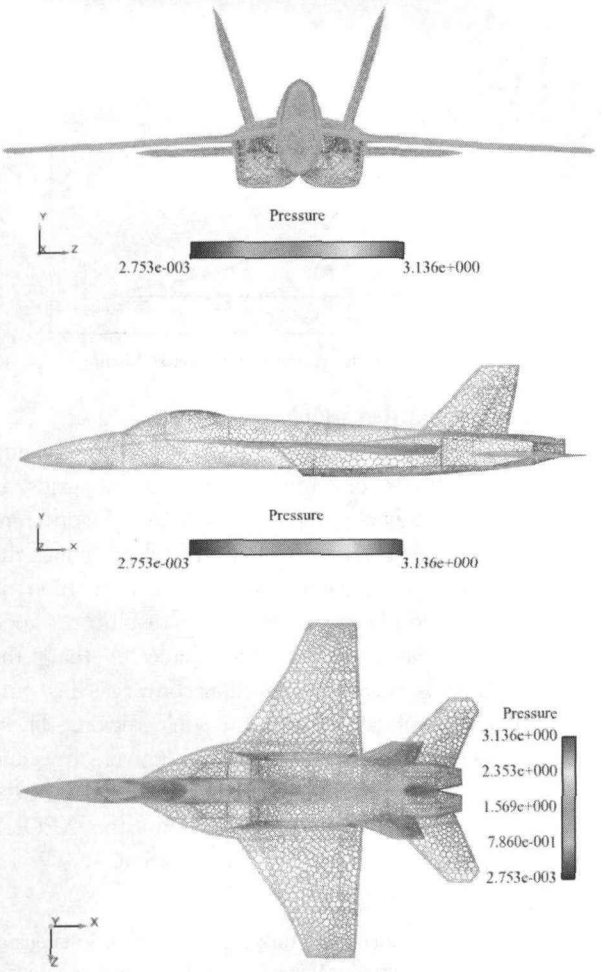

Fig. 8 Honeycomb grids of F-18 aircraft

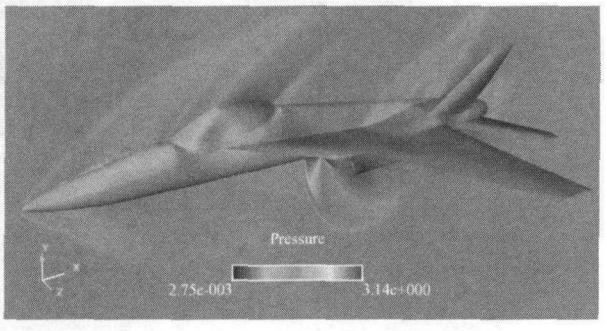

Fig. 9 Pressure contour of F-18 aircraft

Fig. 9 gives the pressure contour on the surface and symmetry plane of the F-18 aircraft. The shock waves are captured clearly by KFVS scheme. In this complex geometry test case, the convergence rate shown in Fig. 10 is slower than the double cone case. It is because of the complex shock structure. The point implicit method is also not the best choice to obtain a fast convergence rate. It indicates that there is still a large room to do some improvements.

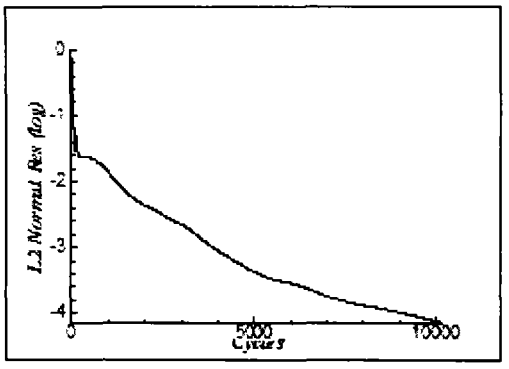

Fig. 10 L2 density residual convergence history

4. Conclusion and Remarking

In this paper, a new kinetic-based solver for solving compressible flows on arbitrary polyhedral grids is presented. The new algorithms are validated by different types of grids. The KFVS scheme is robust while the new RBF based gradient computational method is accurate, the combination of them results in good performance. Numerical results indicate that the honeycomb grids based computation converges fast and exhibits strong robustness in hypersonic region. These results show obvious advantages of universality and flexibility of the solver. So as an accurate and efficient tool for basic aerodynamics calculation, the XPOLY solver could be used in aerospace application.

References

[1] Jameson A, Schmidt W, Turkel E. Numerical solutions of the euler equations by finite volume methods using runge-kutta time-stepping schemes. AIAA Paper 81-1259, AIAA 14th Fluid and Plasma Dynamic Conference, Palo Alto, 1981.

[2] Barth T J, Jespersen D C. The design and application of upwind schemes on unstructured meshes. AIAA Paper 89-0366, 27th Aerospace Sciences Meeting, Reno, Nevada, 1989.

[3] Lohner R, Parikh P. Generation of three-dimensional unstructured grids by the advancing-front method. International Journal for Numerical Methods in Fluids 1988; 8(10): 1135-1149

[4] Mavriplis D J, Multigrid techniques for unstructured meshes. VKI Lecture Series VKI-LS 1995-02, Von Karman Institute for Fluid Dynamics, Rhode-Saint-Genese, Belgium 1995

[5] Frink N T. Upwind scheme for solving the euler equations on unstructured tetrahedral meshes. AIAA Journal, 1992; 1 (1): 70-77.

[6] Mandal J C, Deshpande S M. Kinetic flux vector splitting for euler equations. Computers and Fluids, 1994; 23(2): 447-478.

[7] K Xu. A Gas-kinetic BGK scheme for the navier-stokes equations and its connection with artificial dissipation and godunov method. Journal of Computational Physics, 2001; 1 (171): 289-33

[8] Mavriplis D J. Revisiting the least-squares procedure for gradient reconstruction on unstructured meshes. AIAA paper 2003-3986, AIAA 16th Computational Fluid Dynamics Conference, Orlando, FL, June 2003.

[9] P A Gnoffo. An upwind-biased, point-implicit relaxation algorithm for viscous, compressible perfect-gas flows. NASA TP-2953, Feb. 1990.

[10] Martin D. Buhmann. Radial Basis Functions: Theory and Implementations. Cambridge University. 2003.

[11] Nakahashi K, Saitoh E. Space-marching method on unstructured grid for supersonic flows with embedded subsonic regions. AIAA Journal, 1997; 35(8): 1280-1285.

[12] Schmitt V, F Charpin. Pressure distributions on the ONERA-M6-Wing at transonic mach numbers. Experimental Data Base for Computer Program Assessment. Report of the Fluid Dynamics Panel Working Group 04, AGARD AR138, 1979.

[13] X Zhao, J Lei, S J Zhang. Hypersonic Non-Equilibrium Computations for Ionizing Air. AIAA Paper 2009-1591, 47th AIAA Aerospace Sciences Meeting Including The New Horizons Forum and Aerospace Exposition, Orlando, Florida, 2009.